





# Recycling Construction and Demolition Residues in Clay Bricks

Chiara Zanelli <sup>1</sup>, Elena Marrocchino <sup>2,\*</sup>, Guia Guarini <sup>1</sup>, Alice Toffano <sup>3</sup>, Carmela Vaccaro <sup>3</sup> and Michele Dondi <sup>1</sup>

- <sup>1</sup> CNR-ISTEC, Institute of Science and Technology for Ceramics, 48018 Faenza, Italy; chiara.zanelli@istec.cnr.it (C.Z.); guida.guarini@istec.cnr.it (G.G.); michele.dondi@istec.cnr.it (M.D.)
- <sup>2</sup> Department of Chemical, Pharmaceutical and Agricultural Sciences, University of Ferrara, 44121 Ferrara, Italy
- <sup>3</sup> Department of Physics and Earth Sciences, University of Ferrara, 44122 Ferrara, Italy; alice.toffano@unife.it (A.T.); vcr@unife.it (C.V.)
- \* Correspondence: mrrlne@unife.it; Tel.: +39-339-3807477

**Abstract:** In recent years, the management of construction and demolition residues (CDRs) has become a major challenge for the construction industry due to the increasing volume of waste produced and its associated environmental impact. The aim of this article is to assess the effect of fine-grained fractions (<0.125 mm–0.6–0.125 mm) of construction and demolition residues, obtained by industrial sorting in a CDR processing plant in Rovigo (Italy), on the technological behavior and technical performance of clay bricks. Simulating the brickmaking process on a laboratory scale, it was appraised whether the CDR additions determined any change in the main properties of both fired and unfired bricks, taking a CDR-free brick body as a reference. The results indicated that the use of CDR is technologically feasible. It is possible to obtain, through proper crushing and sorting operations, grain-sized fractions with quite homogenous chemical and mineralogical composition. The residues did affect the compositional properties, porosity and water absorption of the clay bricks. Nevertheless, the characterization of the residual-added semi-finished and fired products highlighted their good technological and mechanical properties, which allowed them to provide performances similar to those of standard bricks manufactured with raw natural materials.



**Citation:** Zanelli, C.; Marrocchino, E.; Guarini, G.; Toffano, A.; Vaccaro, C.; Dondi, M. Recycling Construction and Demolition Residues in Clay Bricks. *Appl. Sci.* **2021**, *11*, 8918. <https://doi.org/10.3390/app11198918>

Academic Editor: Fernanda Andreola

Received: 17 August 2021

Accepted: 21 September 2021

Published: 24 September 2021

**Publisher's Note:** MDPI stays neutral with regard to jurisdictional claims in published maps and institutional affiliations.



**Copyright:** © 2021 by the authors. Licensee MDPI, Basel, Switzerland. This article is an open access article distributed under the terms and conditions of the Creative Commons Attribution (CC BY) license (<https://creativecommons.org/licenses/by/4.0/>).

**Keywords:** construction and demolition residues; clay bricks; technological properties

## 1. Introduction

The construction sector is of strategic importance to the global economy and has a strong influence on three forms of sustainability: environmental, economic and social.

In the EU, construction generates about 10% of Gross Domestic Product (GDP), provides 20 million jobs and has a direct impact on the quality of life of the population [1]. However, in addition to its economic and social benefits, the construction sector creates serious environmental problems during the entire lifecycle of buildings, especially during their operational and end-of-life stages. Infrastructure and building construction and demolition activities consume about 50% of raw materials and account for 33% of the 900 million tons of waste generated in the EU each year [2,3]. Modern societies consume large amounts of raw materials and produce considerable quantities of waste, particularly in the construction sector, generating construction and demolition residue (CDR). In this context, CDR is a major challenge for the construction industry due to the increasing volume of waste produced and its associated environmental impact [4–6].

Construction and demolition residues are the largest waste stream worldwide [7,8] accounting for about 25–30% of the total waste generated in the EU. Therefore, they are considered a priority waste stream, especially in view of the impact caused by their mismanagement [9–11].

There is no particular composition of construction and demolition residues, as they vary depending on the kind of structure, demolition process and construction management systems employed. Generally, CDRs typically include: (1) concrete from superstructures,

(2) bricks, tiles and ceramics from floors, roofs and partition walls and, (3) in lesser quantities, other materials, such as glass, wood, plasterboard, asbestos, metals, plastics and hazardous materials. Most of these wastes are usually disposed of in landfills without any form of recovery or re-use, generating important economic and environmental concerns [12–14]. Because of the negative impact of CDR on the environment and the high rates of waste they produce, the management of CDR has become a priority for sustainable development programs worldwide [14,15]. Its associated environmental effects include land degradation, landfill depletion, carbon and greenhouse gas emissions, water pollution, high energy consumption and resource depletion [16,17].

In light of these environmental challenges, derived from the current linear economy model of “take-make-consume-dispose”, the construction industry requires the implementation of new, enhanced building strategies focused on the problem of CDR [18]. The EU recognizes the need for a sustainable management of waste and of use of natural resources. Consequently, targets were set to increase the re-use, recovery and recycling of non-hazardous CDR across Europe above 70% by 2020, from the current average rate of 47% [19,20].

In this context, the transition to a Circular Economy (CE) is considered a solution, as it would reduce environmental impact while contributing to economic growth [21].

In the framework of the European Green Deal [1], the new Circular Economy Action Plan considers CDR as a priority stream for closing the material loop, thanks to its potential to produce secondary raw materials [22,23], and to contribute towards the goals of the ‘Renovation Wave’.

The re-use and recycling of CDRs has high potential, since most of their components have a high resource value. As the different materials require specific methods of valorization, the most effective management systems suggest the use of appropriate demolition techniques combined with recycling and re-use. Accordingly, glass, wood, asbestos, metals, plastics, hazardous materials, etc. should be separated, obtaining the majority of the inert waste fraction, comprising mainly concrete and masonry remains [12–14,24–28].

Research on the recycling of CDR into ceramic materials is extremely scarce. There are few studies on the technological behavior of CDR in ceramic materials, with the exception of a few studies on lightweight aggregates [29,30] and some papers on clay-based building ceramics [31–40]. In general, these studies concluded that CDRs can be used as major ingredients, but that its processing indications are contradictory (e.g., relevant variation of the firing sintering temperatures). With regard to high-throughput products, such as bricks and tiles, there are only some exploratory studies on the role of CDR in ceramic bodies [39] or, specifically, on the problems connected with asbestos-containing CDR [41]. Furthermore, the focus has recently shifted to niche applications, such as anorthite-mullite-corundum porous ceramics for membranes, with encouraging results [3,26,42–44].

There are no studies concerning the effect of the fine-grained fraction of CDR; therefore we wanted to bridge this gap by assessing their effect on the technological behavior and technical performance of clay bricks. Simulating the brickmaking process on a laboratory scale, it was appraised whether the addition of construction and demolition residues (CDRs) determined any change in the main properties of both fired and unfired products, taking a waste-free brick body as a reference.

## 2. Materials and Methods

### 2.1. Materials

The sampling of the residues studied took place in a construction and demolition residue (CDR) processing plant in Rovigo (Italy). Two different fine-grained fractions ( $R1 \leq 0.125$  mm and  $R2 = 0.6–0.125$  mm) of construction and demolition wastes were selected. Three different types of clays and one type of sand were selected on the basis of their location close to the processing plant: body S (Sila di Rovigo), body G and M (coming from the Vicenza area, Santerna and Fruges) and body C (Colombara sand) (Table 1). The three clays (M-G-S) and the sand (C) are the classic raw material largely used for the

industrial manufacture of bricks and roof tiles. The clays' sources were essentially the following:

- clay S, produced from Holocene fluvial deposits from Villanova del Ghebbo, (Rovigo, Venetian Region);
- clay M, produced from Pleistocene fluvio-glacial deposits from Satena, (Torino, Piemonte Region) [45,46];
- clay G, produced from Holocene alluvial deposits from Fruges, (Ravenna, Emilia Romagna Region) [47].

**Table 1.** Chemical and mineralogical composition, and particle size distribution of the CDR (R1–R2), the sand (C) and the three clays (M–G–S).

Weight %	R1	R2	C	M	G	S	e.u.
Chemical Composition							
SiO <sub>2</sub>	55	36.92	83.7	56.6	53.63	51.54	±0.35
TiO <sub>2</sub>	0.4	0.39	0.1	0.7	0.68	0.73	±0.01
Al <sub>2</sub> O <sub>3</sub>	10.7	8.51	8.13	17.3	13.36	14.47	±0.15
Fe <sub>2</sub> O <sub>3</sub>	3.11	3.41	0.46	6.9	5.26	5.91	±0.07
MnO	0.07	0.08	-	-	0.12	0.11	±0.01
MgO	4.71	7.04	0.18	3	2.79	4.21	±0.02
CaO	11.96	24.02	1.96	3.3	8.46	7.22	±0.01
Na <sub>2</sub> O	1.61	0.95	1.77	0.8	1.26	1.1	±0.01
K <sub>2</sub> O	2.31	1.57	3.55	2.1	2.47	2.82	±0.01
P <sub>2</sub> O <sub>5</sub>	0.16	0.11	-	-	0.13	0.15	±0.01
L.O.I. (1000 °C)	9.68	16.42	0.15	9.3	11.84	11.74	±0.05
Mineralogical composition							
Quartz SiO <sub>2</sub>	30%	17%	58%	27%	28%	32%	±1
Plagioclase (Na,Ca)(Si,Al) <sub>4</sub> O <sub>8</sub>	13%	7%	17%	4%	9%	10%	±1
Orthoclase KAlSi <sub>3</sub> O <sub>8</sub>	6%	6%	19%	t.	t.	t.	±1
Calcite CaCO <sub>3</sub>	13%	26%	3%	6%	15%	5%	±1
Dolomite CaMg(CO <sub>3</sub> ) <sub>2</sub>	13%	24%	-	-	-	10%	±1
Illite-mica K(Al,Mg,Fe) <sub>2</sub> (Si,Al) <sub>4</sub> O <sub>10</sub> (OH) <sub>2</sub> (H <sub>2</sub> O)	10%	3%	2%	23%	23%	26%	±1
Chlorite (Mg,Fe) <sub>3</sub> (Si,Al) <sub>4</sub> O <sub>10</sub> (OH) <sub>2</sub> (Mg,Fe) <sub>3</sub> (OH) <sub>6</sub>	5%	3%	-	11%	9%	6%	±1
Kaolinite Al <sub>2</sub> Si <sub>2</sub> O <sub>5</sub> (OH) <sub>4</sub>	7%	9%	-	9%	3%	-	±1
Smectite + I/S (Na,Ca) <sub>0,3</sub> (Al,Mg) <sub>2</sub> Si <sub>4</sub> O <sub>10</sub> (OH) <sub>2</sub> ·n(H <sub>2</sub> O)	-	-	-	13%	7%	5%	±1
Fe oxyhydroxides Fe(O,OH,H <sub>2</sub> O)	-	-	-	5%	4%	4%	±1
Accessories	3%	5%	1%	2%	2%	2%	±1
Particle size							
Median (µm)	250	260	100	2.3	2.8	1.1	±1
Sand > 64 µm (%)	90	80	65	23	10	3	±1
Silt 4–64 µm (%)	8	13	27	29	47	35	±1
Clay < 4 µm (%)	2	7	8	48	43	62	±1

e.u. = experimental uncertainty; t = trace

## 2.2. Methods

These bodies were characterized through the determination of their chemical composition by XRF–WDS (Philips, Cambridge, UK, PW 1480); their mineralogical composition by XRPD (D8 Advance equipped with a LynxEye detector, Bruker, Karlsruhe Germany); and their particle size distribution by X-ray monitoring of gravity sedimentation (SediGraph 5100, Micromeritics, Norcross, GA, USA).

Nine batches were designed as simple waste plus clay binary mixtures, along with sand + clay taken as the benchmark (SC–GC–MC). Each waste was added in place of sand C as 15%, by weight. The resulting bodies were the S clay (SR1–SR2) and for the M and G clays (MR1–MR2–GR1–GR2).

A laboratory-scale simulation of the industrial manufacturing cycle of clay bricks was carried out through body preparation, shaping, drying, and firing. In particular, the following working phases were carried out:

- (i) clay grinding with a jaw crusher (<20 mm) and a hammer mill (<1 mm). The finest fraction i.e., <6 mm, was subsequently ground on a laboratory scale. The different fractions were thus obtained and were mixed, on the basis of their chemical composition and particle size distribution, with the two most representative CDR batches selected ( $R1 \leq 0.125$  mm and  $R2 = 0.6-0.125$  mm).
- (ii) hand mixing of clay wastes and water, and successive storage for 2 days;
- (iii) plastic extrusion of 100 mm × 20 mm × 10 mm bars, with a pneumatic apparatus without a vacuum;
- (iv) drying at ambient temperature in a non-controlled atmosphere for 48 h and successively with an electric oven at 100 °C overnight;
- (v) firing in an electric chamber kiln, in static air, up to a maximum temperature of 950 °C (for the batches S0-SR1-SR2)–940 °C (for the batches G0-GR1-GR2) and 900 °C (for the batches M0-MR1-MR2), at a heating rate of 50 °C per hour, and with 8 h of dwelling time, for a total cycle of 48 h cold-to-cold. For the three different sets of products, the thermal cycle was chosen in accordance with that used in the industrial production of clay bricks.

Each stage of the bricks' manufacturing process was evaluated. The extrusion stage was evaluated using Atterberg consistency limits [48], in which the plastic limits represent the minimum water content at which the sample can be hand-rolled [49]. The drying was determined by an Adamel apparatus, which measured the weight and length of an 80 mm × 20 mm × 10 mm specimen (taken from an extruded bar with moisture  $W_0$ ) simultaneously, and then allowed to dry at room temperature ( $20 \pm 2$  °C) and relative humidity ( $50 \pm 10\%$ ). The Bigot's curve was drawn by contrasting water loss and linear shrinkage, in order to quantify the extent of the two drying stages ( $W_1$  with shrinkage and  $W_2$  without shrinkage). The drying index was calculated as:  $DSE = W_1/W_0 * \text{drying shrinkage}$  [50].

Moreover, the unfired and fired products were characterized by determining: the level of working moisture [51]; the drying and firing shrinkage [52]; the modulus of rupture of the dry and fired samples [53]; the extent of water absorption, open porosity, and bulk density of the fired samples [54]; the bricks' color (Hunterlab Miniscan MSXP4000).

On the fired products, the disposition toward e efflorescence was analyzed following the indications contained in the UNI 8942/3 and UNI 9730/3 standards [55].

The phase composition of the fired bricks was determined by using X-ray powder diffraction (in the  $10-80^\circ 2\theta$  range, with a point detector equivalent time of 185 s per  $0.02^\circ 2\theta$  scan step (D8 Advance equipped with LynxEye detector, Bruker, Germany) on the powdered samples admixed with 20% corundum as the internal standard in order to quantify the amorphous phase. The quantitative interpretation of the patterns was carried out using RIR-Rietveld refinement (GSAS-EXPGUI software package 2001); the experimental error was within 5% relative [56].

### 3. Results and Discussion

#### 3.1. Characteristics of Raw Materials and Batches

The physical and chemical characterization of the raw materials is presented in Table 1. Their mineralogical composition reflected the coexistence of various clay minerals with quartz, carbonates (calcite and dolomite) and feldspars (alkali feldspar and plagioclase), as well as iron oxyhydroxides. In particular, the clay minerals consisted of illite, chlorite, and kaolinite (expected for S clay), as well as illite/smectite (I/S) interstratified terms [56].

The clays' chemical composition was approximately 55% silica, 15% alumina, 6% calcium and iron, 3% magnesium and 2% potassium oxides.

All clays consisted of quite fine-grained material almost 50% below <4 micron.

The sand C is characterized by a significant coarse fraction (65% up to 64  $\mu\text{m}$ ); as expected, it generally consisted of quartz, plus feldspars and plagioclase, so it was the richest in silica.

The construction and demolition residues (CDRs), which were used as degreasers in the replacement of the sand stored in the processing plants, before being processed, was composed of various elements, such as: bricks (about 50%), incoherent fine materials from mortars and concretes (about 25%), concrete materials (about 20%), metals (about 3%), plastic, paper, rubber parts and wood (in total about 1%) and asphalt (about 1%). The sampling of the residues under study took place in heaps of materials previously industrially processed (through sieving, etc.) in the landfill.

Overall, the CDRs were composed mainly of quartz, dolomite, calcite, mica, and kaolinite; therefore, they turned out to be quite rich in alkali, alumina, calcium,  $\text{Fe}_2\text{O}_3$  and  $\text{MgO}$ . Compared to R1, the residue R2 is characterized by a greater amount of calcite + dolomite (about 50%) and a lower content of quartz and plagioclase.

In terms of particle size, the CDRs displayed a coarser distribution than the sand C (R1-2 median particle size 250  $\mu\text{m}$ -sand C 100  $\mu\text{m}$ ).

As concerns all the batches, the replacement of CDRs produced, in general, a decrease in silica and potassium with respect to the three references, MC-GC-SC. At the same time,  $\text{Al}_2\text{O}_3$ ,  $\text{Fe}_2\text{O}_3$ ,  $\text{MgO}$  and  $\text{CaO}$  increased, while the other components fluctuated according to the residues that were added (Table 2). As expected, the CDRs induced a variation in the particle size distribution batches; the replacement of the sand with the CDRs involved an increase of more than double the median particle size.

### 3.2. Technological Behaviour during Extrusion and Drying

The evaluation was made both by simulating the brickmaking process and by measuring the level of plasticity according to the Atterberg consistency limits. The replacement of the fractions of CDR1-2 with sand consistently led to an increase in the Atterberg limits. This effect could be linked to the presence of clay minerals in the CDRs, which therefore lead to the absorption of a greater amount of water.

The Atterberg limits were reflected in the working moisture data, that is, the water that was needed to humidify the mixtures. The replacement with the CDR fractions required a greater amount of mixing water; this was not only due to the presence of the clay minerals, but also to the presence of a higher amount of carbonate (lime). In fact, in the residues, the quantity of carbonate was conspicuous compared to the quantity in the sand; moreover, its content was greater for R2 than for R1.

As observed in Table 3 and in Figure 1, the drying shrinkage decreased as the bulk density decreased and, in particular, the introduction of the CDR fractions led to a decrease in density (except for the sample MR1) compared to the mixtures with sand. The mixtures containing the R2 fraction displayed density values lower than R1, which was probably related to the particle size difference; R2 is slightly coarser than R1.

In general, for the three sets of batches, the dry flexural strength obtained with the R1 aggregate showed higher values than the products obtained with R2. This effect was due to their different particle size distribution (R1 is finer than R2) and also to the difference in their mineralogical composition (R1 has a lower carbonate content than R2).

### 3.3. Technological Behaviour after Firing

Tables 4 and 5 present the results related to the firing behavior of ceramics batches. In all the products, the introduction of CDR fractions leads to an increase in both water absorption and firing shrinkage. Taking into account the flexural strength of the firing products, a decrease of MOR in the CDR products would be expected given the greater porosity extent and lower density appearing.

**Table 2.** Formulation, chemical and mineralogical composition, and particle size distribution of the batches.

Weight (%)	MC	MR1	MR2	GC	GR1	GR2	SC	SR1	SR2	e.u.
Clay M	85	85	85	85	85	85	85	85	85	±0.3
Clay G	-	-	-	-	-	-	-	-	-	±0.3
Clay S	-	-	-	-	-	-	-	-	-	±0.3
Sand C	15	-	-	15	-	-	15	-	-	±0.3
CDR R1	-	15	-	-	15	-	-	15	-	±0.3
CDR R2	-	-	15	-	-	15	-	-	15	±0.3
Chemical composition										
SiO <sub>2</sub>	65.62	62.21	59.72	64.28	60.87	58.38	62.21	58.80	56.31	±0.35
TiO <sub>2</sub>	0.67	0.72	0.73	0.67	0.72	0.73	0.72	0.77	0.77	±0.01
Al <sub>2</sub> O <sub>3</sub>	17.43	18.00	17.75	14.10	14.66	14.42	15.16	15.72	15.47	±0.15
Fe <sub>2</sub> O <sub>3</sub>	6.54	6.98	7.08	5.14	5.59	5.69	5.76	6.21	6.31	±0.07
MnO	-	0.01	0.01	0.12	0.13	0.13	0.11	0.12	0.12	±0.01
MgO	2.84	3.60	4.08	2.72	3.47	3.96	4.08	4.84	5.33	±0.02
CaO	3.39	5.09	7.43	8.45	10.15	12.50	7.25	8.95	11.29	±0.01
Na <sub>2</sub> O	1.02	1.02	0.92	1.48	1.48	1.39	1.33	1.33	1.23	±0.01
K <sub>2</sub> O	2.50	2.35	2.25	2.91	2.77	2.67	3.25	3.10	3.00	±0.01
P <sub>2</sub> O <sub>5</sub>	-	0.03	0.02	0.13	0.15	0.15	0.14	0.17	0.16	±0.01
Mineralogical composition										
Quartz SiO <sub>2</sub>	32	27	26	33	28	26	36	32	30	±1
Plagioclase (Na,Ca)(Si,Al) <sub>4</sub> O <sub>8</sub>	6	5	4	10	10	9	11	10	10	±1
Orthoclase KAlSi <sub>3</sub> O <sub>8</sub>	3	1	1	3	1	1	3	1	1	±1
Calcite CaCO <sub>3</sub>	6	7	9	13	15	17	5	6	8	±1
Dolomite CaMg(CO <sub>3</sub> ) <sub>2</sub>	-	2	4	0	2	4	9	10	12	±1
Illite-mica K(Al,Mg,Fe) <sub>2</sub> (Si,Al) <sub>4</sub> O <sub>10</sub> (OH) <sub>2</sub> (H <sub>2</sub> O)	20	21	20	20	21	20	22	24	23	±1
Chlorite (Mg,Fe) <sub>3</sub> (Si,Al) <sub>4</sub> O <sub>10</sub> (OH) <sub>2</sub> (Mg,Fe) <sub>3</sub> (OH) <sub>6</sub>	9	10	10	8	8	8	5	6	6	±1
Kaolinite Al <sub>2</sub> Si <sub>2</sub> O <sub>5</sub> (OH) <sub>4</sub>	8	9	9	3	4	4	-	1	1	±1
Smectite + I/S (Na,Ca) <sub>0,3</sub> (Al,Mg) <sub>2</sub> Si <sub>4</sub> O <sub>10</sub> (OH) <sub>2</sub> ·n(H <sub>2</sub> O)	11	11	11	6	6	6	4	4	4	±1
Fe oxyhydroxides Fe(O,OH,H <sub>2</sub> O)	4	4	4	3	3	3	3	3	3	±1
Accessories	2	2	2	2	2	2	2	2	2	±1
Particle size distribution										
Median (µm)	17	39	41	17	40	41	16	38	40	±0.5
Sand >64 µm (%)	29	33	32	18	22	21	12	16	15	±0.5
Silt 4–64 µm (%)	29	26	27	44	41	42	34	31	32	±0.5
Clay <4 µm (%)	42	41	42	38	37	38	54	53	54	±0.5

e.u. = experimental uncertainty.

**Table 3.** Plasticity and drying behavior of batches.

Parameter	Unit	MC	MR1	MR2	GC	GR1	GR2	SC	SR1	SR2	e.u.
Atterberg plastic limit (PL)	wt%	20.3	20.3	21.2	26.9	28.2	30.1	24.2	25.5	25.8	±0.1
Atterberg liquid limit (LL)	wt%	36.0	38.5	40.7	51.7	53.4	53.7	46.1	46.6	47.4	±0.1
Atterberg plastic index (PI)	wt%	15.7	18.1	19.5	24.8	25.3	23.8	21.9	21.2	21.7	±0.1
Working moisture (WI)	%	20.4	20.6	21.2	25.6	26.2	26.7	26.7	27.9	29.9	±0.1
Bigot moisture (W <sub>0</sub> )	wt%	20.4	20.6	21.2	25.6	26.2	26.7	26.7	27.9	29.9	±0.1
Weight loss with shrinkage (W <sub>1</sub> )	%	47.0	55.0	50.5	48.0	53.0	49.5	39.5	46.5	43.0	±0.1
Weight loss without shrinkage (W <sub>2</sub> )	%	53.0	45.0	49.5	52.0	47.0	50.5	60.5	53.5	57.0	±0.1
Drying ratio (W <sub>1</sub> /W <sub>0</sub> ) (WR)	1	2.30	2.67	2.38	1.88	2.02	1.85	1.48	1.67	1.44	±0.01
Drying index (WR × LDS) (DSI)	1	12.65	14.69	12.14	13.16	13.53	11.29	10.06	11.36	9.36	±0.05
Bulk density (BD)	g/cm <sup>3</sup>	1.995	2.003	1.955	1.932	1.917	1.891	1.916	1.892	1.859	±0.005
Drying shrinkage (LDS)	cm/m	5.5	5.5	5.1	7.0	6.7	6.1	6.8	6.8	6.5	±0.1
Drying sensitivity index (IDS) (LDS × W <sub>1</sub> /100)	1	2.6	3.0	2.6	3.4	3.6	3.0	2.7	3.2	2.8	±0.03
Dry modulus of rupture (MOR-D)	MPa	8.3	8.7	8.0	9.4	10.0	8.4	8.6	9.7	7.2	±0.5

e.u. = experimental uncertainty.



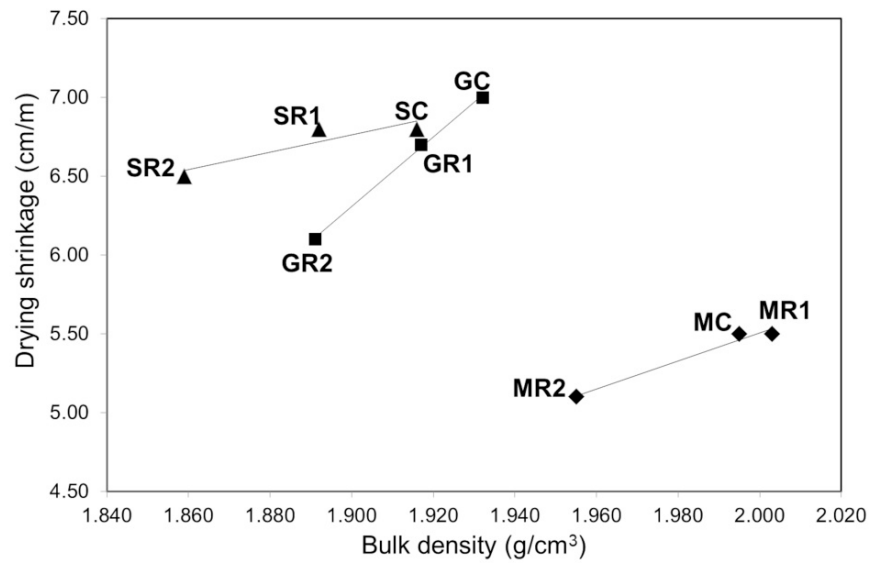


Figure 1. Correlation between bulk density versus drying shrinkage of unfired products.

Table 4. Firing behavior of batches.

		MC	MR1	MR2	GC	GR1	GR2	SC	SR1	SR2	e.u.
Firing maximum temperature	°C	900	900	900	940	940	940	950	950	950	-
Firing shrinkage (FS)	cm/m	0.5	0.5	1.1	0.4	0.7	1.2	0.5	0.5	1.0	±0.1
Modulus of rupture (MOR-F)	MPa	11.0	10.6	8.3	14.8	15.5	15.6	16.3	18.1	18.0	±0.5
Water absorption (WA)	%wt	9.7	10.5	11.0	14.9	15.8	17.3	14.2	14.9	16.3	±0.1
Open porosity (OP)	%vol	19.3	20.6	21.4	26.6	28.1	30.2	25.8	26.7	28.5	±0.2
Bulk density (FBD)	g/cm <sup>3</sup>	1.992	1.957	1.942	1.780	1.786	1.746	1.815	1.792	1.746	±0.01
Normalized strength (MOR-N)	MPa	13.6	13.3	10.6	20.2	21.5	22.3	22.0	24.7	25.2	±1
Brightness (L*)	1	52.97	51.27	50.34	56.31	55.98	55.22	57.08	55.86	56.47	±0.5
Red (+) Green (-) (a*)	1	22.67	23.15	23.70	21.26	21.55	21.85	22.36	23.10	23.20	±0.5
Yellow (+) Blue (-) (b*)	1	26.95	26.08	27.04	26.29	27.33	27.79	27.57	28.81	29.45	±0.5
Color difference (ΔE*)	1	ref	1.96	2.81	ref	1.10	1.96	ref	1.89	2.14	±0.2

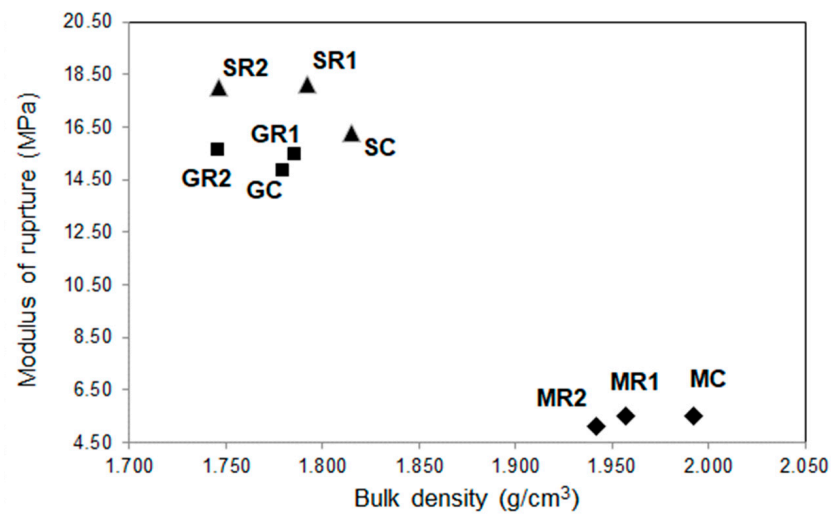
e.u. = experimental uncertainty, ref = reference.

Table 5. Phase composition of fired clay bricks.

Weight %	MC	MR1	MR2	GC	GR1	GR2	SC	SR1	SR2	e.u.
Quartz	28.9	35.3	33.6	30	19.9	29.4	32	32	19.4	±0.5
Plagioclase	4.7	9.0	5.4	39.7	24.7	33.3	34.9	36.1	22.4	±0.2
Illite-mica	4.7	5.9	3.9	6.2	4.2	7	4.2	4.8	4.0	±0.2
K-Feldspar	2.4	2.7	2.2	5.6	3	5.8	4.3	7.7	2.9	±0.2
Clinopyroxene	8.4	8.2	8.5	5.6	6.9	12.3	16.1	11.5	9.2	±0.1
Hematite	2.3	3.2	3.6	3	2.3	4.1	2.7	3.5	2.2	±0.1
Amorphous phase	48.7	35.7	42.8	9.8	39	8.3	5.8	4.3	39.9	±1

e.u. = experimental uncertainty.

Analyzing the modulus of rupture, expect to find lower values in samples with CRDs compared to batches containing sand, given the greater porosity and lower density. As observes in Figure 2 an unexpected trend for clays S and G occur. their modulus of rupture is similar, but the bulk density decreases with the increase G in flexural strength.



**Figure 2.** Correlation between bulk density and modulus of rupture of fired products.

This behavior was once again linked to differences in mineralogical composition; the residues were richer in the carbonate fraction than sand, which during firing lead to the formation of porosity.

In all the samples, there was an absence of or, at least, a poor degree of efflorescence, indicating that the CDRs has no detrimental effect compared to the reference sand.

The only mixtures that demonstrated poor efflorescence were those made with clay G; however, they could be seen both in the reference mixtures and in the products with CDRs. Therefore, it is plausible to suppose that it is the clay itself that has an aptitude for efflorescence (Figure 3 [57]).

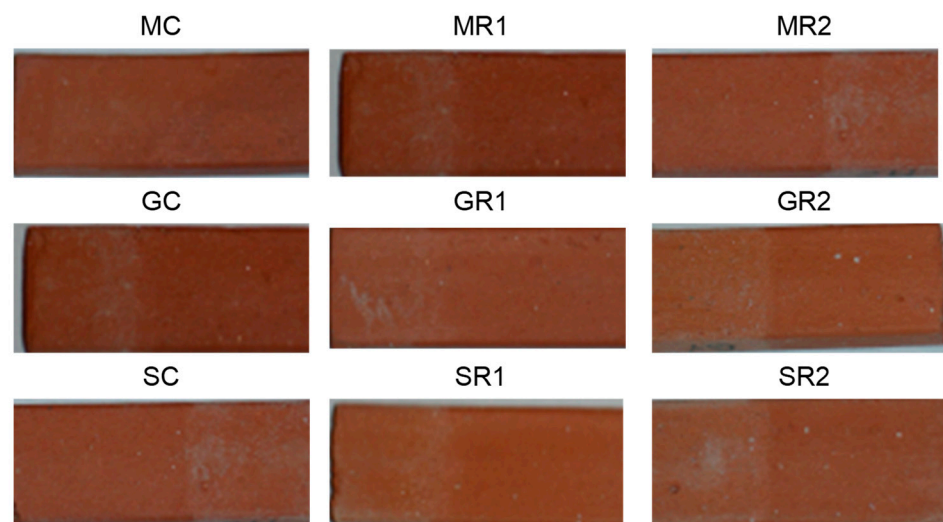


**Figure 3.** Efflorescence in fired products.

The introduction of CDRs resulted in a more yellow-green color in the fired products, with a decrease in brightness compared to the reference sample with sand.

The mineralogical composition of the bricks included quartz, plagioclase, clinopyroxene, muscovite, alkali-feldspar, hematite and a variable quantity of amorphous phase. It was consistent with that of the raw materials. All the batches contained residual phases that were already present in the clays and in the CDRs (i.e., quartz, feldspar, hematite and muscovite) and also contained new phases that formed during firing, including plagioclase, which was derived from calcite decomposition and the reaction with the silicate matrix.



In detail, the following results were obtained:

- in the samples containing clay M, the introduction of the CDRs did not significantly modify the mineralogical composition. There was an increase in plagioclase (especially with R1), which was clearly to the detriment of the amorphous phase.
- in the samples containing clay S, the introduction of the R2 residue led to considerable variations in the quantitative ratios of the phases, with a decrease in the content of quartz, plagioclase and k feldspar and a consequent increase in the amorphous phase.
- in the samples containing clay G, the introduction of residue R1 led to a net decrease of quartz and k feldspar and a conspicuous increase in the amorphous phase.

The main physical and technological properties were normalized with respect to the reference bodies (GC, MC, SC) in order to verify the influence of the residue substitution on the three sets of batches. In Figure 4, the radar graphs show the multiple data points and the variation between them. What emerges is that the two CDRs clearly affected the technological behavior of the fired and unfired products in different ways. However, no evident variation was observed in relation to the three different clays used. This highlights the crucial role that the particle size distribution and mineralogical composition of CDRs play in their design for use as ceramic raw materials. If the main physical and technological properties of the products with CDRs are compared with those used in the industrial production of bricks manufactured with natural raw materials, then the values fell within the ranges of the optimal parameters (Table 6).

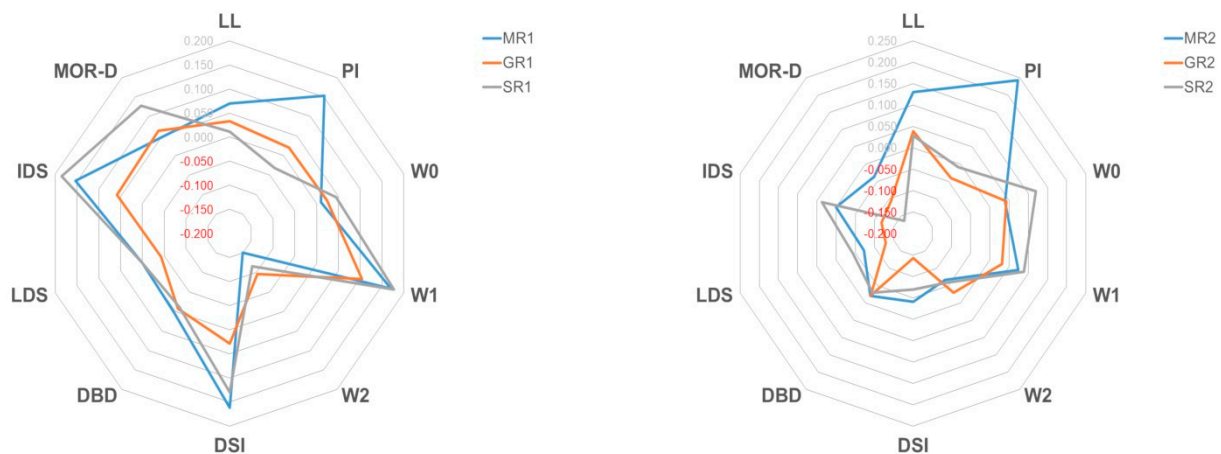


Figure 4. Radar graph of the main physical and technological properties normalized respect to the reference bodies (MC-SC-GC) for addition of waste R1 (left) or R2 (right).

Table 6. Comparison between the main physical and technological properties.

Parameter	Reference	MC	MR1	MR2	GC	GR1	GR2	SC	SR1	SR2
Working moisture %	20–30	21	21	21	26	26	27	27	28	30
Bulk density g/cm <sup>3</sup>	1.85–2.10	2.0	2.0	2.0	1.9	1.9	1.9	1.91	1.9	1.9
Drying shrinkage cm/m	3–10	6	6	5	7	7	6	7	7	7
Dry modulus of rupture MPa	8–15	8	9	8	9	10	8	9	10	7
Firing maximum temperature °C			900			940			950	
Firing shrinkage cm/m	<1.5	0.5	0.5	1.1	0.4	0.7	1.2	0.5	0.5	1.0
Fired modulus of rupture MPa	10–25	11	11	8	15	16	16	16	18	18
Water absorption %wt	10–25	10	11	11	15	16	17	14	15	16

#### 4. Conclusions

In clay bricks, the addition of the two fine-grained fractions (R1 ≤ 0.125 mm and R2 = 0.6–0.125 mm) of construction and demolition residues is technologically feasible. The two fractions of CDR clearly affect the technological behavior of both unfired and fired

clay bricks in different ways. Their particle size distribution and mineralogical composition play a crucial role in their design for use as raw materials in the production of clay bricks.

When compared with the clay bricks commonly used in the industrial practice, the main physical and technological performances (working moisture, bulk density, drying/firing shrinkage and dry/fired modulus of rupture, water absorption) of clay bricks with CDRs showed values that fell within the range of optimal parameters.

**Author Contributions:** Conceptualization: C.Z., E.M., C.V. and M.D.; methodology: C.Z., G.G. and M.D.; validation: C.Z., G.G., E.M., C.V. and M.D.; formal analysis: C.Z., G.G. and A.T.; investigation: C.Z., E.M., G.G., A.T., C.V. and M.D.; resources: C.V. and M.D.; data curation: C.Z., G.G., E.M. and M.D.; writing—original draft preparation: C.Z., E.M., G.G., A.T., C.V. and M.D.; supervision, C.Z., E.M., C.V. and M.D.; project administration: C.Z. and E.M. All authors have read and agreed to the published version of the manuscript.

**Funding:** This research received no external funding.

**Institutional Review Board Statement:** Not applicable.

**Informed Consent Statement:** Not applicable.

**Data Availability Statement:** Not applicable.

**Conflicts of Interest:** The authors declare no conflict of interest.

## References

1. European Commission. COM 2019, 640. The European Green Deal. Available online: <https://pdc.minambiente.it/it/norme/politicaenormativa/politica-ambientale/politica-europea/com-2019-640-final-del-11122019-il> (accessed on 20 October 2020).
2. European Commission. *Study on Modelling of the Economic and Environmental Impacts of Raw Material Consumption*; Technical Report; European Commission: Brussels, Belgium, 2014; pp. 2014–2478.
3. Bravo, M.; de Brito, J.; Pontes, J.; Evangelista, L. Durability performance of concrete with recycled aggregates from construction and demolition waste plants. *Constr. Build. Mater.* **2015**, *77*, 357–369. [[CrossRef](#)]
4. López Ruiz, L.A.; Roca, R.X.; Gassó, D.S. The circular economy in the construction and demolition waste sector—A review and an integrative model approach. *J. Clean. Prod.* **2020**, *248*, 119–238. [[CrossRef](#)]
5. Geng, S.; Wang, Y.; Zuo, J.; Zhou, Z.; Du, H.; Mao, G. Building life cycle assessment research: A review by bibliometric analysis. *Renew. Sustain. Energy Rev.* **2017**, *76*, 176–184. [[CrossRef](#)]
6. Ghisellini, P.; Ji, X.; Liu, G.; Ulgiati, S. Evaluating the transition towards cleaner production in the construction and demolition sector of China: A review. *J. Clean. Prod.* **2018**, *195*, 418–434. [[CrossRef](#)]
7. Jin, Q.; Yang, L.; Poe, N.; Huang, H. Integrated processing of plant-derived waste to produce value-added products based on the biorefinery concept. *Trends Food Sci. Technol.* **2018**, *74*, 119–131. [[CrossRef](#)]
8. Tam, V.W.Y.; Tam, C.M. A review on the viable technology for construction waste recycling. *Resour. Conserv. Recycl.* **2006**, *47*, 209–221. [[CrossRef](#)]
9. Iodice, S.; Garbarino, E.; Cerreta, M.; Tonini, D. Sustainability assessment of Construction and Demolition Waste management applied to an Italian case. *Waste Manag.* **2021**, *128*, 83–98. [[CrossRef](#)] [[PubMed](#)]
10. Duan, H.; Wang, J.; Huang, Q. Encouraging the environmentally sound management of C&D waste in China: An integrative review and research agenda. *Renew. Sustain. Energy Rev.* **2015**, *43*, 611–620.
11. Marzouk, M.; Azab, S. Environmental and economic impact assessment of construction and demolition waste disposal using system dynamics Resources. *Conserv. Recycl.* **2014**, *82*, 41–49. [[CrossRef](#)]
12. Gupta, V.; Chai, H.K.; Lu, Y.; Chaudhary, S. A state of the art review to enhance the industrial scale waste utilization in sustainable unfired bricks. *Constr. Build. Mater.* **2020**, *254*, 119220. [[CrossRef](#)]
13. Gavali, H.R.; Bras, A.; Faria, P.; Ralegaonk, R.V. Development of sustainable alkali-activated bricks using industrial wastes. *Constr. Build. Mater.* **2019**, *215*, 180–191. [[CrossRef](#)]
14. Seco, A.; Omer, J.; Marcelino, S.; Espuelas, S.; Prieto, E. Sustainable unfired bricks manufacturing from construction and demolition wastes. *Constr. Build. Mater.* **2018**, *167*, 154–165. [[CrossRef](#)]
15. Esa, M.R.; Halog, A.; Rigamonti, L. Developing strategies for managing construction and demolition wastes in Malaysia based on the concept of circular economy. *J. Mater. Cycles Waste Manag.* **2017**, *19*, 1144–1154. [[CrossRef](#)]
16. Akanbi, L.A.; Oyedele, L.O.; Akinade, O.O.; Ajayi, A.O.; Davila Delgado, M.; Bilal, M.; Bello, S.A. Salvaging building materials in a circular economy: A BIM-based whole-life performance estimator. *Resour. Conserv. Recycl.* **2018**, *129*, 175–186. [[CrossRef](#)]
17. Ding, Z.; Wang, Y.; Zou, P.X.W. An agent based environmental impact assessment of building demolition waste management: Conventional versus green management. *J. Clean. Prod.* **2016**, *133*, 1136–1153. [[CrossRef](#)]
18. Jaillon, L.; Poon, C.S. Life cycle design and prefabrication in buildings: A review and case studies in Hong Kong. *Autom. Constr.* **2014**, *39*, 195–202. [[CrossRef](#)]

19. European Commission. Directive 2008/98 of 19 November 2008 on waste and repealing certain Directives. *Off. J. Eur. Union* **2008**, *34*, 99–126.
20. Pacheco-Torgal, F. Eco-efficient construction and building materials research under the EU Framework Programme Horizon 2020. *Constr. Build. Mater.* **2014**, *51*, 151–162. [[CrossRef](#)]
21. Lieder, M.; Rashid, A. Towards circular economy implementation: A comprehensive review in context of manufacturing industry. *J. Clean. Prod.* **2016**, *115*, 36–51. [[CrossRef](#)]
22. European Commission. COM 2020 98. *A New Circular Economy Action Plan. For a Cleaner and More Competitive Europe*; European Commission: Brussels, Belgium, 2020.
23. European Commission. COM 2020 662. *Renovation Wave for Europe—Greening Our Buildings, Creating Jobs, Improving Lives*; European Commission: Brussels, Belgium, 2020.
24. Seco, A.; Urmeneta, P.; Prieto, E.; Marcelino, S.; García, B.; Miqueleiz, L. Estimated and real durability of unfired clay bricks: Determining factors and representativeness of the laboratory tests. *Constr. Build. Mater.* **2017**, *131*, 600–605. [[CrossRef](#)]
25. Contreras, M.; Teixeira, S.R.; Lucas, M.C.; Lima, L.C.N.; Cardoso, D.S.L.; da Silva, G.A.C.; Gregório, G.C.; de Souza, A.E.; dos Santos, A. Recycling of construction and demolition waste for producing new construction material (Brazil case-study). *Constr. Build. Mater.* **2016**, *123*, 594–600. [[CrossRef](#)]
26. Silva, C.; Pereira, P.M.; Lopes, M.L. Recycled Construction and Demolition Wastes as filling material for geosynthetic reinforced structures. Interface properties. *J. Clean. Prod.* **2016**, *124*, 299–311.
27. Vegas, I.; Broos, K.; Nielsen, P.; Lambertz, O.; Lisbona, A. Upgrading the quality of mixed recycled aggregates from construction and demolition waste by using near-infrared sorting technology. *Constr. Build. Mater.* **2015**, *75*, 121–128. [[CrossRef](#)]
28. Silva, R.V.; de Brito, J.; Dhir, R.K. Properties and composition of recycled aggregates from construction and demolition waste suitable for concrete production. *Constr. Build. Mater.* **2014**, *65*, 201–217. [[CrossRef](#)]
29. Wang, C.; Wu, J.Z.; Zhang, F.S. Development of porous ceramsite from construction and demolition waste. *Environ. Technol.* **2013**, *34*, 2241–2249. [[CrossRef](#)]
30. Mueller, A.; Schnell, A.; Rübner, K. The manufacture of lightweight aggregates from recycled masonry rubble. *Constr. Build. Mater.* **2015**, *98*, 376–387. [[CrossRef](#)]
31. Liu, Z.; Chen, Q.; Xie, X.; Xue, G.; Du, F.; Ning, Q.; Huang, L. Utilization of the sludge derived from dyestuff-making wastewater coagulation for unfired bricks. *Constr. Build. Mater.* **2011**, *25*, 1699–1706. [[CrossRef](#)]
32. Oti, J.E.; Kinuthia, J.M. Stabilised unfired clay bricks for environmental and sustainable use. *Appl. Clay Sci.* **2012**, *58*, 52–59. [[CrossRef](#)]
33. Miqueleiz, L.; Ramirez, F.; Oti, J.E.; Seco, A.; Kinuthia, J.M.; Oreja, I.; Urmeneta, P. Alumina filler waste as clay replacement material for unfired brick production. *Eng. Geol.* **2013**, *163*, 68–74. [[CrossRef](#)]
34. Zhang, L. Production of bricks from waste materials—A review. *Constr. Build. Mater.* **2013**, *47*, 643–655. [[CrossRef](#)]
35. Li, G.; Xu, X.; Chen, E.; Fan, J.; Xiong, G. Properties of cement-based bricks with oyster-shells ash. *J. Clean. Prod.* **2015**, *91*, 279–287. [[CrossRef](#)]
36. Acchar, W.; Silva, J.E.; Segadaes, A.M. Increased added value reuse of construction waste in clay based building ceramics. *Adv. Appl. Ceram.* **2013**, *112*, 487–493. [[CrossRef](#)]
37. Schackow, A.; Stringari, D.; Senff, L.; Correia, S.L.; Segadaes, A.M. Influence of fired clay brick waste additions on the durability of mortars. *Cem. Concr. Compos.* **2015**, *62*, 82–89. [[CrossRef](#)]
38. Oti, J.E.; Kinuthia, J.M.; Robinson, R.B. The development of unfired clay building material using Brick Dust Waste and Mercia mudstone clay. *Appl. Clay Sci.* **2014**, *102*, 148–154. [[CrossRef](#)]
39. Da Silva, V.M.; Costa Góis, L.; Duarte, J.B.; da Silva, J.B.; Acchar, W. Incorporation of Ceramic Waste into Binary and Ternary Soil-Cement Formulations for the Production of Solid Bricks. *Mater. Res.* **2014**, *17*, 326–331. [[CrossRef](#)]
40. Contreras Llanes, M.; Romero Pérez, M.; Gázquez González, M.J.; Bolívar Raya, J.P. Construction and demolition waste as recycled aggregate for environmentally friendly concrete paving. *Environ. Sci. Pollut. Res.* **2021**. [[CrossRef](#)]
41. Gualtieri, A.F. Recycling asbestos-containing material (ACM) from construction and demolition waste (CDW). In *Handbook of Recycled Concrete and Demolition Waste*; Woodhead Publishing: Sawston, UK, 2016; pp. 500–525.
42. Cabalar, A.F.; Abdulnafa, M.D.; Karabash, Z. Influences of various construction and demolition materials on the behavior of a clay. *Environ. Earth Sci.* **2016**, *75*, 841. [[CrossRef](#)]
43. Dos Reis, G.S.; Cazacliu, B.G.; Cothenet, A.; Poullain, P.; Wilhelm, M.; Sampaio, C.H.; Lima, E.C.; Ambros, W.; Torrenti, J.M. Fabrication, microstructure, and properties of fired clay bricks using construction and demolition waste sludge as the main additive. *J. Clean. Prod.* **2020**, *258*, 120733. [[CrossRef](#)]
44. He, Z.; Shen, A.; Wu, H.; Wang, W.; Wang, L.; Yao, C.; Wu, J. Research progress on recycled clay brick waste as an alternative to cement for sustainable construction materials. *Constr. Build. Mater.* **2021**, *274*, 122113. [[CrossRef](#)]
45. Dondi, M.; Ercolani, G.; Fabbri, B.; Guarini, G.; Marsigli, M.; Mingazzini, C. Major deposits of brick clays in Italy. Part 1: Geology and composition. *Tile Brick Int.* **1999**, *15*, 230–237.
46. Dondi, M.; Ercolani, G.; Fabbri, B.; Guarini, G.; Marsigli, M.; Mingazzini, C. Major deposits of brick clays in Italy Part 2: Technological properties and uses. *Tile Brick Int.* **1999**, *15*, 360–370.
47. Dondi, M.; Fabbri, B.; Vincenzi, S. Raw materials for the heavy-clay industry in Emilia-Romagna and Marche (central-northern Italy). *Geol. Carpathica-Clays* **1999**, *22*, 83–90.

48. ASTM. *D4318 Standard Test Methods for Liquid Limit, Plastic Limit, and Plasticity Index of Soils*; American Society for Testing and Materials: West Conshohocken, PA, USA, 1998.
49. Bain, J.A. A plasticity chart as an aid to the identification and assessment of industrial minerals. *Clay Miner.* **1970**, *9*, 1–17. [[CrossRef](#)]
50. Dondi, M.; Marsigli, M.; Venturi, I. Sensibilità all'essiccamento e caratteristiche porosimetriche delle argille italiane per laterizi (Drying sensitivity and porosimetric characteristics of the Italian brick clays). *Ceramurgia* **1998**, *28*, 1–8.
51. ASTM. *C324 Test Method for Free Moisture in Ceramic Whiteware Clays*; American Society for Testing and Materials: West Conshohocken, PA, USA, 1992.
52. ASTM. *C326 Test Method for Drying and Firing Shrinkage of Ceramic Whiteware Clays*; American Society for Testing and Materials: West Conshohocken, PA, USA, 1997.
53. ASTM. *C674 Test Method for Flexural Properties of Ceramic Whiteware Materials*; American Society for Testing and Materials: West Conshohocken, PA, USA, 1994.
54. ASTM. *C373 Test Method for Water Absorption, Bulk Density, Apparent Porosity, and Apparent Specific Gravity of Fired Whiteware Products*; American Society for Testing and Materials: West Conshohocken, PA, USA, 1994.
55. Dondi, M.; Fabbri, B.; Guarini, G.; Marsigli, M.; Mingazzini, C. Soluble salts and efflorescence in structural clay products: A scheme to predict the risk of efflorescence. *Bol. Soc. Esp. Ceram. Vidr.* **1997**, *36*, 619–629.
56. Gualtieri, A.F. Accuracy of XRPD QPA using the combined Rietveld\_RIR method. *J. Appl. Cryst.* **2000**, *33*, 267–278. [[CrossRef](#)]
57. Slaný, M.; Jankovič, L.; Madejová, J. Structural characterization of organo-montmorillonites prepared from a series of primary alkylamines salts: Mid-IR and near-IR study. *Appl. Clay Sci.* **2019**, *176*, 11–20. [[CrossRef](#)]